Measurement of Force Vector Field of Robotic Finger using Vision-based Haptic Sensor

Katsunari Sato, Kazuto Kamiyama, Hideaki Nii, Naoki Kawakami, and Susumu Tachi,

The University of Tokyo, Japan

Abstract—It is expected that the use of haptic sensors to measure the magnitude, direction, and distribution of a force will enable a robotic hand to perform dexterous manipulations. Therefore, we have developed a new type of finger-shaped haptic sensor that can measure a three-dimensional force vector field over a contact surface. The sensor consists of a transparent elastic body, two layers of internal blue and red markers, and a CCD camera to capture the movements of the markers. Using the elastic theory, we can calculate the force vector field from the captured movements of the markers. However, the elastic theory cannot be applied to the finger-shaped sensor because of its complicated shape. Therefore, we use actual measurements for the calibration in order to develop a prototype of the sensor. Then, we evaluate its basic performance. The result shows that the sensor performance can be improved further, and the sensor can be successfully used in a robotic hand.

I. INTRODUCTION

HAPTIC information acquired through the fingertips is important for human since it allows them to manipulate an object dexterously. The object can be grasped in a stable manner using haptic information such as the reflective force, frictional force, and point of contact with the object. Robotic systems use a similar methodology. In order to pick up, move, or lay down an object, a robotic hand requires haptic information. Therefore, robotic hands require haptic sensors to manipulate objects dexterously. Recently, two principal types of haptic sensors have been invented for robotic hands [1] [2]: a force vector sensor that measures three- or six-dimensional force at a point and a force field sensor that measures the distribution of a one-dimensional force.

The objective of our research is to achieve dexterous manipulation in various activities such as rolling clay between the fingertips by using a robotic hand with a haptic sensor (Fig. 1). We have laid down three requirements for the haptic sensor of the robotic hand. First, the sensor should be able to measure

Katsunari Sato, Hideaki Nii, Naoki Kawakami, and Susumu Tachi are affiliated with the Graduate School of Information and Technology, The University of Tokyo, Japan;;e-mail: (Katsunari_Sato,Hideaki_Nii)@ipc.i.u-tokyo.ac.jp,(kawakami, tachi)@star.t.u-tokyo.ac.jp.

Kazuto Kamiyama is affiliated with the Research Center for Advanced Science and Technology, The University of Tokyo, Japan; e-mail: kazuto@hal.   rcast.u-tokyo.ac.jp.

the magnitude, direction, and distribution of an applied force. Conventional sensors mainly measure only one or two of these parameters. However, all three parameters are essential for stable grasping and dexterous manipulation. Second, the size of the sensor should be small. In order to set many haptic sensors in a humanoid robot hand, it is preferable to use compact sensors. Finally, the sensor should be a high-performance device. In order to obtain accurate haptic information, high magnitude, spatial, and temporal resolutions are better.
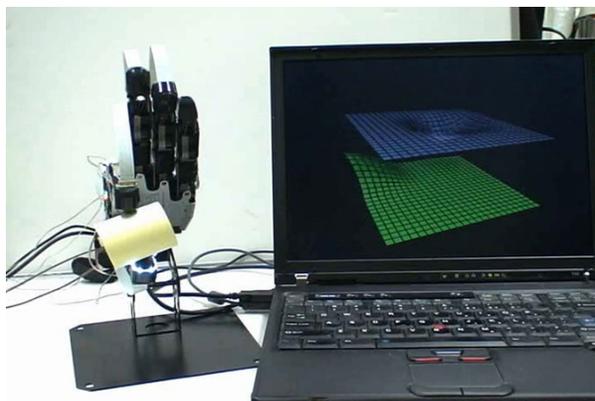

Fig. 1. Example of manipulation by robotic hand using our fingertip sensor. The blue and green surfaces shown in the laptop display represent the information measured by the sensors mounted on the index finger and the thumb of the robotic hand, respectively.

The first requirement can be satisfied by integrating many force vector sensor elements [3] [4]. However, the use of many sensors can complicate the sensor structure and decrease the sensor performance. Ferrier et. al. have proposed another approach to satisfy the first requirement [5]. They have developed a small tactile sensor to measure the force vector field. However, this sensor requires a complex processing method to acquire the direction of force, leading to inaccuracy and instability.

In order to satisfy all the abovementioned requirements, we have created a finger-shaped haptic sensor that can measure a three-dimensional force vector field applied on its surface. The technology used by this sensor is the same as that used in the vision-based haptic sensor developed by us [6]. This

sensor has a simple structure; hence, it satisfies the second and third requirements, i.e., having small size and high resolution.

In this paper, we present the measurement theory, configuration, and calibration method of the finger-shaped haptic sensor. In addition, we evaluate its accuracy when it is used as a force vector sensor and a force field sensor.

II. FINGER-SHAPED HAPTIC SENSOR

A. Theory for measurement of force vector field

In order to enable the finger-shaped haptic sensor to measure the force vector field, we have applied the technology used in the vision-based haptic sensor. This sensor consists of a transparent elastic body with two layers of a marker matrix and a color CCD camera. When a force is applied to the surface, the markers move as shown in Fig. 2. The movements of the markers are captured by the camera. We calculate the center of the markers before and after application of the force. Therefore, we can record the movements of markers and calculate the applied force using the elastic theory [7].
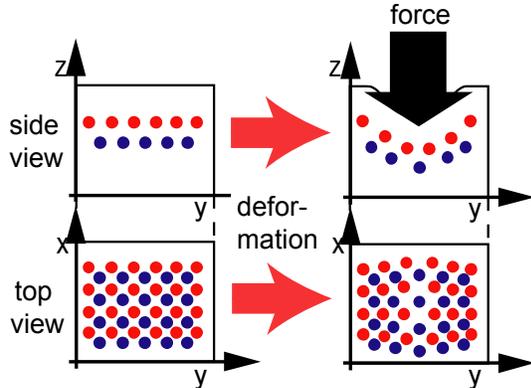

Fig. 2. Movements of markers in elastic sensor body caused by force applied to sensor surface [6].

We use two suppositions to calculate the force vector field from the movements of the markers. The first supposition is that the sensor is a semi-infinite elastic body. The second supposition is that the deformation of the elastic body is linear. On the basis of these suppositions, the relationship between the movement of marker and force is given by equation (1) as follows:

$$u = Hf . \tag{1}$$

$$u = \begin{bmatrix} u_{Rx} \\ u_{Ry} \\ u_{Bx} \\ u_{By} \end{bmatrix}, H = \begin{bmatrix} h_{Rxx}, h_{Ryx}, h_{Rzx} \\ h_{Rxy}, h_{Ryy}, h_{Rzy} \\ h_{Bxx}, h_{Byx}, h_{Bzx} \\ h_{Bxy}, h_{Byy}, h_{Bzy} \end{bmatrix}, f = \begin{bmatrix} f_x \\ f_y \\ f_z \end{bmatrix}$$

In this equation, u indicates the two-dimensional movement vectors of the red and blue markers captured by the camera, f is the three-dimensional force vector, and H is the conversion matrix. The elements of H are calculated by using the elastic theory. We obtain f from u by solving the inverse problem [8] of equation (1).

$$f = \left(H^T H\right)^{-1} H^T u . \tag{2}$$

It should be noted that the vision-based sensor uses a single camera to capture the movements of the two layers of markers. In order to calculate the three-dimensional force vector, it is necessary to measure the movements of the markers in a three-dimensional manner. A stereo camera is suitable for capturing the movements of the markers. However, the use of a stereo camera increases the size of the sensor and the difficulty in calibrating the camera. Hence, to overcome these problems, we use two layers of markers and one camera.

This vision-based haptic sensor does not require any electronic components such as resistors or capacitors. Hence, it is easy to adapt the shape and size of the sensor to that of the fingertip. In addition, further developments in camera technology will result in improved spatial and temporal resolution of the sensor. The elastic body of the sensor provides an added advantage. The elasticity enables the sensor to appropriately measure the haptic information by reproducing the physical interaction involved in the sense of touch. Furthermore, the sensor is highly durable.

B. Design of sensor

We construct the fingertip sensor for the robotic hand by applying vision-based technology.

The configuration of the sensor is shown in Fig. 3. The elastic body and CCD camera are attached to the plastic base of the robotic hand. The elastic body is made from transparent silicon rubber. The shape of the elastic body is partly spherical and partly cylindrical; hence, it resembles a human fingertip. There are blue and red markers on the surface of the elastic body. Because the sensor uses vision-based technology, light from the environment produces noise. Therefore, the surface of the sensor is covered by a black sheet made from the silicon rubber. In addition, to capture the marker movements clearly, they are illuminated by an LED mounted near the camera. We use a camera with a wide-angle lens so that the camera can capture all the markers.

C. Calibration method

In conventional vision-based haptic sensors, the applied force is calculated from the movement of the markers using equation (1). However, equation (1) has been derived on the basis of two suppositions. These suppositions are not applicable to the finger-shaped haptic sensor. Hence, we estimate the elements of the conversion matrix H from actual

measurements.

Figure 4 shows the algorithm for the construction of H. First, a force is applied on the surface of the sensor along three directions; the components of the force along the three directions are denoted by f_x, f_y, and f_z. Then, we measure the force elements caused by applying the force as follows:

$$f_n = \begin{bmatrix} f_{xx}, f_{xy}, f_{xz} \\ f_{yx}, f_{yy}, f_{yz} \\ f_{zx}, f_{zy}, f_{zz} \end{bmatrix} \quad (3)$$

where f_{mn} indicates the m-directional element of force when n-directional force is applied. Next, we capture the movements of the markers u_n. The x-directional marker movements of a marker are given by equation (4).

$$u_n = \begin{bmatrix} u_{xx}, u_{xy}, u_{xz} \end{bmatrix} \quad (4)$$

where u_{mn} indicates the m-directional movement of marker when n-direction force is applied. Using f_n and u_n, we can calculate the elements of matrix H as follows:

$$h_n = u_n f_n^{-1} \qquad \left(h_n = \begin{bmatrix} h_x, h_y, h_z \end{bmatrix} \right) \quad (5)$$
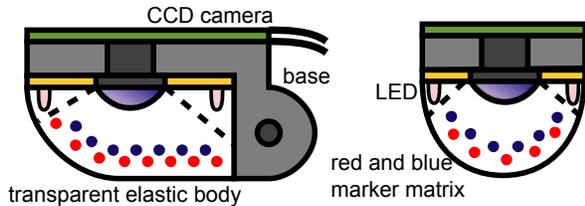

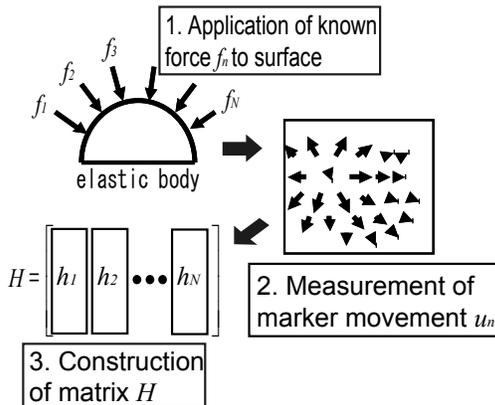Fig. 3. Configuration diagram of finger-shaped vision-based haptic sensor.

Fig. 4. Algorithm for construction of conversion matrix H. The elements of H are calculated from the measured force f_n and the movements of the markers denoted by u_n.

Figure 5 shows the apparatus used for the construction of matrix H. We push the sensor surface by using a probe. The probe edge is spherical and the diameter is 3.0 mm. The probe is mounted on a six-axis force sensor to measure the magnitude of the applied force. Further, we use an xyz stage to control the applied force. We first apply a force along the z-direction and then apply suitable forces along the x- and y-directions.
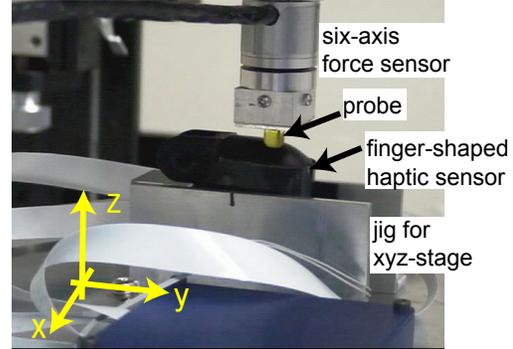

Fig. 5. Image of apparatus used for construction of conversion matrix H.

D. Construction of prototype of finger-shaped haptic sensor

We have constructed a prototype of the finger-shaped haptic sensor. The dimensions of the transparent elastic body of the prototype are $16 \times 16 \times 10$ mm³. The elastic body is made from silicon rubber (Shin-Etsu Chemical Co., KE-109). The camera is a custom-made one comprising a video compression unit and four image capturing units (ViewPLUS Inc.). The resolution of each image is 640×480 pixels. The centers of the markers are tracked with sub-pixel accuracy. The frame rate of the camera is 60 fps. Figure 6 shows the captured images of the markers. To capture the markers clearly, their diameters are set to 0.5 mm (approximately 15 pixels). Moreover, in order to prevent the overlapping of the red and blue markers, they are separated by a distance of 2.5 mm (Fig. 6, left). The red and blue markers are placed at depth of 0.5 and 2.0 mm, respectively, from the surface of the sensor. We print the markers using the silk-screen printmaking technique. The markers are made from silicon rubber and a colorant.

The calibrated positions of the forces are shown in Fig. 6 (right). In the prototype, the markers are separated by a distance of 2.5 mm. Therefore, we apply a force at 25 points on the surface of the sensor. The points are also separated by a distance of 2.5 mm. The magnitude of the applied force is approximately 100 gf.

Figure 7 shows the constructed prototype and the calculated force vector field. When the sensor surface comes in contact with an object, it measures the corresponding force vector fields.
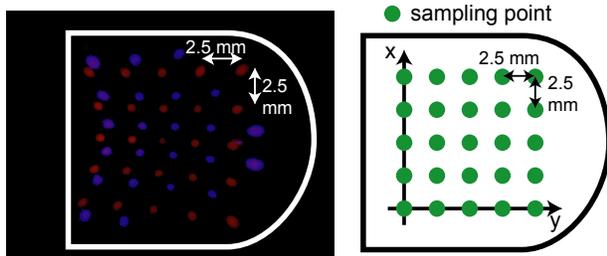
Fig. 6. Images of markers captured by camera (left) and points used for sampling force (right).
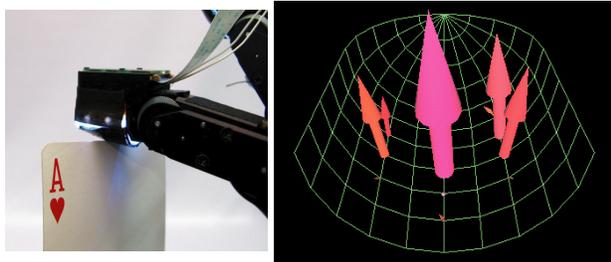

Fig. 7. Images of constructed sensor (left) and captured force vector field (right).

III. EVALUATION

The finger-shaped haptic sensor can be used both as a force vector sensor and as a force field sensor. Therefore, we evaluate the basic performance of the constructed prototype using the following four criteria: the accuracy of measurement, the resolution of the force magnitude when it is used as a force vector sensor, the spatial resolution when it is used as a force field sensor, and the time required for calculation. The apparatus used in the evaluation of the environment is the same as that used for calibration (Fig. 6).

A. Measurement accuracy

The force vector field is calculated from the movements of the centers of the markers captured by the camera. Therefore, an error that occurs while capturing the movements of the markers may produce noise in the measurement of the force. In this section, we evaluate the accuracy of the measurement of the movements of the markers when no force is applied to the surface of the sensor.

We capture two images of the markers when no force is applied. Then, we displace the markers in one of the images by 5 pixels along the x-direction. The displacement vectors of the markers are calculated using these two images. Table I shows the average and the standard deviation of the x- and y-displacements of the red and blue markers. The result shows that the movements of the markers are measured with subpixel accuracy.

B. Resolution of magnitude

The finger-shaped haptic sensor can be used as a force vector sensor. We evaluate the resolution of the force

magnitude along the three directions: x, y, and z. Each directional force, f_x, f_y, and f_z, is represented by a one-dimensional force vector and the summations of the force denoted by F_x, F_y, and F_z, respectively, are calculated as shown in equation (6).

$$
\begin{aligned}
F_x &= \sum_{k=1}^{n} f_x(k) \\
F_y &= \sum_{k=1}^{n} f_y(k) \\
F_z &= \sum_{k=1}^{n} f_z(k)
\end{aligned}
\tag{6}
$$

We examine the resolution and linearity of the measured force vectors by comparing the measured force F with the applied force. The applied force is measured by using the six-axis force sensor and the controlled xyz stage. In this evaluation, we apply a force using a cylindrical probe with a diameter of 10 mm.

To investigate the resolution of magnitude in the x- and y-direction, we first applied a force of 200 gf along the z-direction. We then applied the force along the x- or y-direction with magnitudes in the range of 20-200 gf by increasing in steps of 20 gf. To investigate the resolution along the z-direction, we applied a force along the z-direction with magnitudes in the range of 20-200 gf by increasing in steps of 20 gf. The values obtained from the sensor are recorded. The measurement procedure is repeated 5 times for each direction.

The graphs shown in Fig. 8 present the results of the evaluation. The horizontal and vertical axes represent the applied force and the measured force, respectively. The dots show the results of each trial. From these results, it is observed that the maximum resolution of magnitude is 30 gf in each direction. Thus, the linearity of the sensor is confirmed.

TABLE I
MEASUREMENT OF MARKER MOVEMENT

Marker	Direction	Average (pixel)	Std. Deviation (pixel)
Red	+x	4.87	0.14
	+y	0.03	0.14
Blue	+x	4.95	0.13
	+y	0.00	0.10

C. Spatial resolution

The finger-shaped haptic sensor can be used to measure a force field. In this section, we evaluate the spatial resolution of the sensor. For the evaluation, we obtain the magnitude of each force vector when a force is applied at a certain point on the surface of the elastic body. The magnitude of the force vector f is calculated as shown in equation (7).

$$
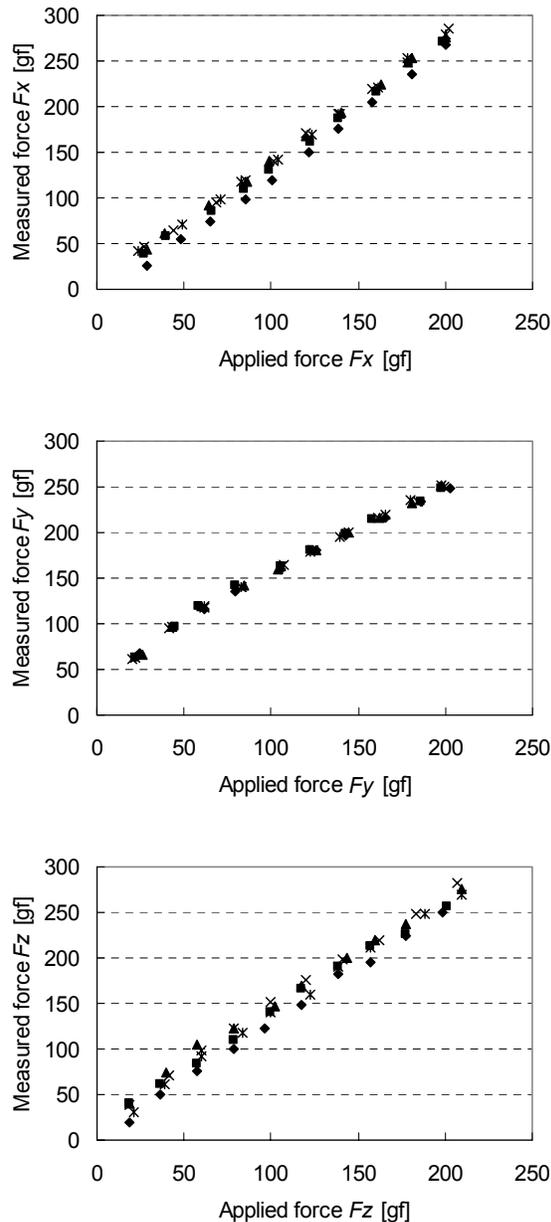f = \sqrt{f_x^2 + f_y^2 + f_z^2}
\tag{7}
$$

Fig. 8. Relation between applied force and measured force in x-direction (top), y-direction (middle), and z-direction (bottom).

It should be noted that the sampling interval is not sufficiently small to evaluate the spatial resolution. Therefore, we adopt the following procedure to evaluate the spatial resolution. Two adjacent sampling points on the sensor surface are selected. The distance between these two points is subdivided into n points, and a known force is applied in the z-direction at each point. Then, the force vectors at each point are calculated by considering each point as the origin. A graph

is constructed by plotting the distance from each origin and the calculated force magnitude on the horizontal and vertical axes, respectively. By using the method explained above, the density of the points in the sampling region is increased. The spatial resolution of the force distribution can be obtained from the slope of the graph.

The magnitude of the force applied in the z-direction is fixed at 200 gf. The diameter of the probe used to apply the force is 3.0 mm. The adjacent sampling points are located at the center and the edge of the area in which the force field is measured. The actual sampling interval is 2.5 mm, and the distance between adjacent points is subdivided into intervals of 0.5 mm. We evaluate the spatial resolution at both the center and the edge of the sensor surface and in both the x- and y-directions.

Figure 9 shows the results of the experiment. The first graph shows the results obtained by applying a force at the center of the sensor. The second graph shows the results obtained by applying a force at the edge of the sensor. The values plotted on the vertical axis are normalized using the maximum value of the force magnitude. The dots in the graphs represent the points at which the force is applied (x [mm], y [mm]).

From the graphs in Fig. 9, it can be observed that the full width half maximum is approximately 5 mm. Therefore, the spatial resolution of the force is estimated to be approximately 5.0 mm. These results are identical to those obtained in the evaluations at other positions and directions. Therefore, the complicated shape of the sensor does not affect the spatial resolution. The discontinuous result around the central position is caused by an error in the calculation of the pseudo-inverse matrix in equation (2).

D. Calculation time

For dexterous manipulation, we need to obtain haptic information from multiple sensors. Therefore, we must process a large amount of information from different sensors simultaneously. In this section, we evaluate the calculation times for the finger-shaped haptic sensor and four sensors.

The calculation time is obtained from the frequency of the CPU. The speed of the processor used in the PC in this experiment is 2.8 GHz (Intel® Pentium®D processor). The program runs on Windows XP SP2. The accuracy of measurement is 1 μs. The calculation time is measured from 100 trials, and the average and standard deviation of the calculation time are shown in Table II.

In this prototype, the camera unit captures four images at 67 fps. Therefore, the PC must calculate the force vector fields of the four sensors within 16 ms. The result satisfies this requirement even when we process the information from the four sensors simultaneously.
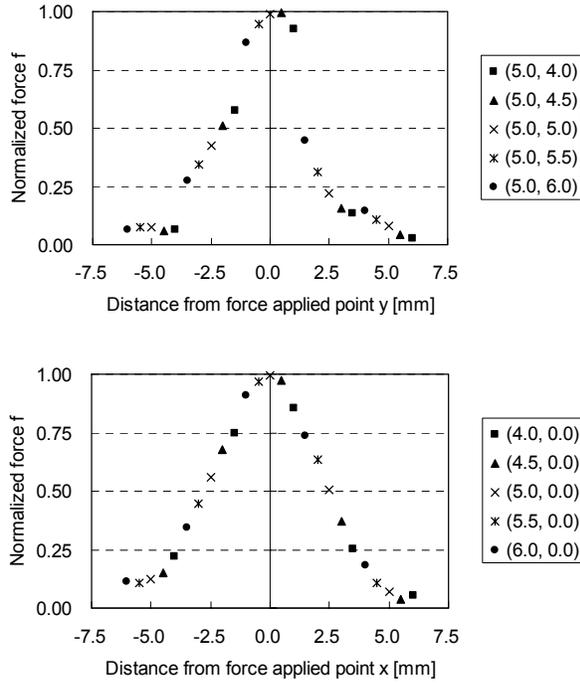
Fig. 9. Force measured by high-density sampling. The first and second graphs show the results of the application of force at the center and the edge of the sensor, respectively.

TABLE II
CALCULATION TIME

Number of sensors	Average [μs]	Std.Deviation [μs]
1	545	56
4	2159	43

IV. DISSCUSSION

The finger-shaped haptic sensor exhibits linear response and its force magnitude resolution is 30 gf in all the three directions. Moreover, the spatial resolution of the sensor is 5.0 mm in the x- and y-directions at any point. These results show that the finger-shaped haptic sensor can be used as a both force vector sensor and a force field sensor.

The results also indicate a possibility for further improvement in the performance of the sensor. The spatial resolution of the sensor is identical to that obtained from the sampling theory. Therefore, the spatial resolution can be improved by reducing the diameter of the markers and the distance between them. For example, to obtain a spatial resolution similar to that of the human fingertip (approximately 2.0mm [9]) for the sensor, the distance between the markers and the diameter of each marker should be 0.2 and 1 mm, respectively. In the prototype, the marker diameter is 0.5 mm or 10-20 pixels, and the error in the measurement of the marker movement is 0.15 pixel. Therefore, we can reduce the size of the markers and the distance between

them in order to realize the desired specifications.

The time resolution of the sensor can also be improved. In the prototype sensor, the calculation time is less than 2.5 ms even after using four sensors. Therefore, a time resolution of 400 Hz can be realized by improving of the frame rate of the camera.

The finger-shaped haptic sensor is capable of performing basic functions and can be improved further. Therefore, we believe that the implementation of this haptic sensor will enable robotic hands to perform dexterous manipulations.

V. CONCLUSION

In order to enable a robotic hand to perform dexterous manipulations, we developed a finger-shaped haptic sensor that can measure a three-dimensional force vector field. We applied the technology used in the vision-based haptic sensor developed by us to the finger-shaped haptic sensor. Because of the complicated shape of the finger-shaped sensor, we used actual measurements for the calibration in order to develop a prototype of the sensor. We then evaluated the basic performance of the sensor.

The results of the evaluation imply that further improvement in the resolution of the sensor is possible. Hence, we will further modify the finger-shaped sensor to enable a robotic hand to manipulate objects and realize dexterous manipulation by using the information on the force vector field.

REFERENCES

[1] H.R. Nicholls, M. H. Lee, "A Survey of Robot Tactile Sensing Technology," Int. J. Robotics Research, Vol. 8, pp. 3-30, 1989.
[2] M. H. Lee, H. R. Nicholls, "Tactile Sensing for Mechatronics – A State of the Art Survey," Mechatronics, Vol. 9, pp. 1-31, 1999.
[3] J. G. Silva, A. A. Carvalho, D. D. Silva, "A Strain Gauge Tactile Sensor for Finger-mounted Applications," on IEEE Trans. On Instruction and Measurement, Vol. 51, No. 1, pp. 18-22. 1991.
[4] M. Ohoka, Y. Mituya, K. Hattori, I. Higashioka, "Data Conversion Capability of Optical Tactile Sensor Featuring an Array of Pyramidal Projections," IEEE International Conference on Multisensor Fusion and Integration for Intelligent Systems, pp. 573-580, 1996.
[5] N. J. Ferrier, R. W. Brockett, "Reconstructing the Shape of a Deformable Membrane from ImageData," The International Journal of Robotics Research, Vol. 19, No. 9, pp. 795-816, 2000.
[6] K. Kamiyama, H. Kajimoto, N. Kawakami, S.Tachi, " Evaluation of a Vision-based Tactile Sensor," In Proc. of International Conference on Robotics and Automation (ICRA2004), 2004, pp. 1542-1547.
[7] L. D. Landau, E.M.Lifshitz, "Theory of Elasticity," ButterworthHeinemann, 1985.
[8] W. Menke, "Geophysical Data Analysis: Discrete Inverse Theory," Academic Press Inc., 1989.
[9] E. R. Kandel, J. H. Schwartz, T. M. Jessel, "Principles of Neural Science, 4th Edition," McGraw-Hill, 2000.